

## Origin of Lorentzian pulses in deterministic chaos

J. E. Maggs and G. J. Morales

*Physics and Astronomy Department, University of California, Los Angeles, California 90095, USA*

(Received 6 March 2012; published 13 July 2012)

Pulses having a temporal Lorentzian shape arise naturally from topological changes in flow trajectories or phase-space orbits associated with deterministic chaos. The pulses can appear as random intermittent events in the time series of observable quantities, and they are the cause of exponential frequency power spectra previously observed in magnetically confined plasmas and various nonlinear systems.

DOI: [10.1103/PhysRevE.86.015401](https://doi.org/10.1103/PhysRevE.86.015401)

PACS number(s): 52.25.Gj, 05.45.Ac, 52.25.Fi, 52.25.Xz

In a recent letter [1] it was emphasized that detailed measurements in a basic linear plasma machine [2,3] and in a toroidal stellarator confinement device [4] established a link between an exponential frequency dependence of the fluctuation power spectrum, i.e.,  $P(\omega) \propto \exp(-2\omega\tau)$ , and Lorentzian temporal pulses having the functional form

$$L(t) = A/[1 + (t - t_0)^2/\tau^2], \quad (1)$$

with  $A$  being the peak amplitude at time  $t_0$  and  $\tau$  being the pulse width. The insight obtained from experiments in magnetically confined plasmas also provided a physical interpretation for the well-established concept within the fluid and nonlinear dynamics communities [5–16] that an exponential frequency spectrum is an inherent signature of deterministic chaos [17]. The connection established by the plasma experiments ruled out that the exponential feature is a statistical property (e.g., a canonical distribution); rather, it is the imprint of individual intermittent events with a unique shape. It is natural to question why pulses emerging from a chaotic system should have a Lorentzian shape. In fact, some researchers [18–21] expect that such pulses should more closely follow a Gaussian form or other distorted shapes determined by random events. This Rapid Communication answers this question by illustrating explicitly the origin of Lorentzian pulses as chaotic dynamics near the separatrix boundaries of elliptic regions in flow fields or, more generally, near the limit cycles of attractors in nonlinear dynamics models. Two explicit examples are considered, a bifurcation given by a potential field appropriate for drift waves in a plasma and a case from the classic example of deterministic chaos, the Lorenz model [22].

A two-dimensional (2D) bifurcation, the Lorentzian bifurcation, is introduced that is appropriate for describing  $E \times B$  motion arising from the interaction of two or more drift waves created by pressure gradients in the edge region of magnetically confined plasmas. This bifurcation has trajectories whose  $y$  components  $y(t)$  have a Lorentzian character. The flow field of the bifurcation has a single stationary point, and the flow trajectories (or streamlines) are contours of constant potential. The potential and attendant velocity field have the form

$$\begin{aligned} \Phi(x, y) &= -(x^2 + c^2)y^2 + by; \\ v_x &= 2y(x^2 + c^2) - b; \quad v_y = -2xy^2, \end{aligned} \quad (2)$$

with  $b$  and  $c$  being real numbers. The stationary point in the flow occurs at the point  $x = 0$  and  $y = b/2c^2$ . The Jacobian

matrix, evaluated at the stationary point in the flow, has zero trace and eigenvalues,  $\omega = \pm ib/c$ . The potential value at the stationary point is a maximum and has the positive value  $b^2/4c^2$ . The form of the potential is illustrated in Fig. 1(a) for  $b = 1, c = 1$ .

Solutions for the trajectories  $[x(t), y(t)]$  of the potential flow field are divided into three topological classes: closed orbits, the separatrix, and unbounded orbits. Closed orbits occur for potential values greater than zero ( $\Phi_0 > 0$ ), and their explicit form is

$$\begin{aligned} x(t) &= \frac{-(b^2 - 4c^2\Phi_0)^{1/2}}{2\sqrt{\Phi_0}} \sin(2\sqrt{\Phi_0}t); \\ y(t) &= \frac{2\Phi_0}{b + (b^2 - 4c^2\Phi_0)^{1/2} \cos(2\sqrt{\Phi_0}t)} \end{aligned} \quad (3)$$

A closed orbit is illustrated by the contour labeled  $\Phi_0 = 0.0475$  in Fig. 1(a). The separatrix is the boundary between closed and unbounded orbits and is delineated by two curves:

$$x = 0 \forall y \in (-\infty, \infty); \quad x(t) = bt, \quad y(t) = \frac{b/c^2}{1 + b^2t^2/c^2}. \quad (4)$$

Comparing Eq. (4) to Eq. (1), it is apparent that the width of the Lorentzian associated with the separatrix is  $\tau_s = c/b$ , and its amplitude is  $b/c^2$ . The separatrix is illustrated by the dashed lines in Fig. 1(a). Unbounded orbits occur for negative potential ( $\Phi_0 < 0$ ) and have the form

$$\begin{aligned} x(t) &= 2q \sinh(\sqrt{|\Phi_0|}t) \cosh(\sqrt{|\Phi_0|}t); \\ y(t) &= \frac{2\sqrt{|\Phi_0|}}{4q \sinh^2(\sqrt{|\Phi_0|}t) + d}, \end{aligned} \quad (5)$$

where

$$q^2 = (b^2 + 4|\Phi_0|c^2)/4|\Phi_0|; \quad d = 2(|q| - b/2\sqrt{|\Phi_0|}). \quad (6)$$

An unbounded orbit is illustrated by the contour labeled  $\Phi_0 = -0.2405$  in Fig. 1(a).

The  $y$  component of these trajectories  $y(t)$  is all Lorentzian in some respect. The trajectory along the upper part of the separatrix is a single Lorentzian pulse, the closed orbits are an infinite train of Lorentzian pulses, and the unbounded orbits can be well approximated by the difference of two Lorentzians. A function with the form  $\delta^2/[1 + \sqrt{1 - \delta^2} \cos(\omega t)]$  can be

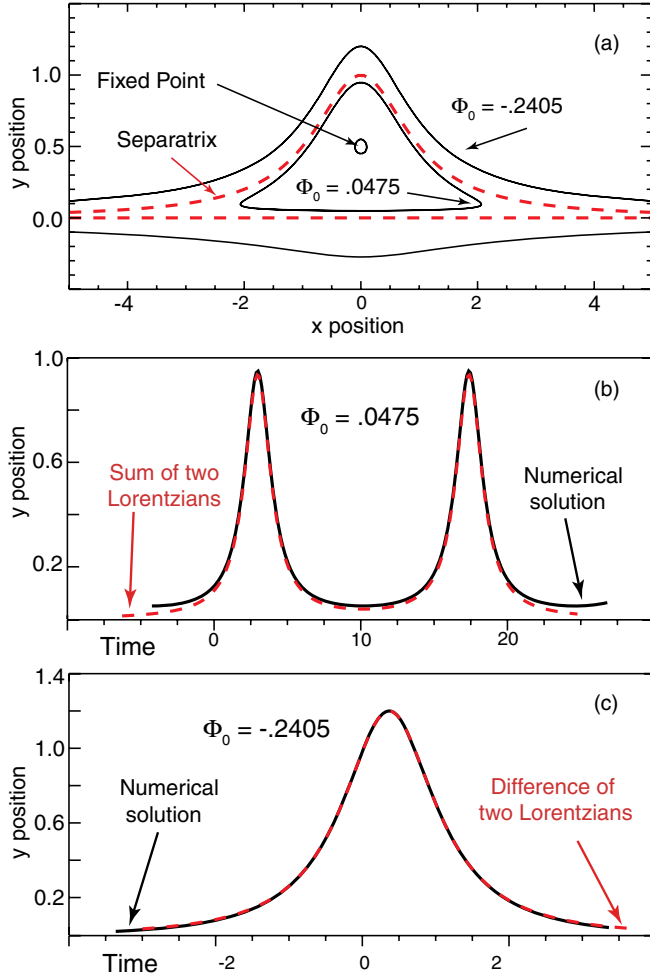


FIG. 1. (Color) (a) Potential contours of the Lorentzian bifurcation with parameter values  $b = c = 1$ . (b) Numerical solution along the contour  $\Phi_0 = 0.0475$  compared to the sum of two Lorentzians. (c) Numerical solution along the contour  $\Phi_0 = -0.2405$  compared to the difference of two Lorentzians.

written as an infinite sum of equal width, equal amplitude Lorentzian pulses [23], so that, for the closed orbits in Eq. (3),

$$y(t) = 1/(c\tau) \sum_{n=-\infty}^{n=\infty} 1/\{1 + [(t - n\pi/\sqrt{\Phi_0})/\tau]^2\}, \quad (7)$$

with  $\tau = \tanh^{-1}(2c\sqrt{\Phi_0}/b)/2\sqrt{\Phi_0}$ . The superposition of two Lorentzian pulses with amplitudes  $1/c\tau = 0.933$  and widths  $\tau = 1.07$  and separated in time by  $\pi/\sqrt{\Phi_0} = 14.4$  are compared in Fig. 1(b) to a fourth order Runge-Kutta integration along the contour with  $\Phi_0 = 0.0475$ , shown in Fig. 1(a). The two-pulse fit is very good but slightly low in amplitude because it consists of only two pulses and not an infinite series. The distance between peaks in the sum of pulses in Eq. (7),  $\pi/\sqrt{\Phi_0}$ , becomes infinite as  $\Phi_0 \rightarrow 0$ , and a single pulse remains, with the same width and amplitude as the separatrix trajectory of Eq. (4). The unbounded orbits occur along contours with a negative potential and can be approximated by the difference

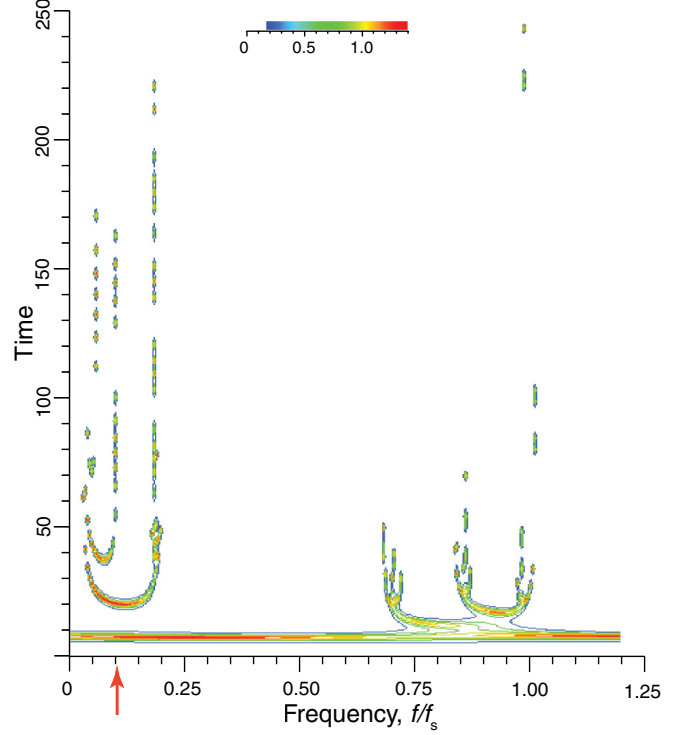


FIG. 2. (Color) Contours of  $y(t)$ , with amplitude values indicated by the color bar, as a function of modulation frequency and time. Chaotic behavior is observed in two frequency intervals.

of two Lorentzian pulses (assuming  $\tau_1 < \tau_2$ ),

$$\begin{aligned} y(t) &\approx A_1/(1 + t^2/\tau_1^2) - A_2/(1 + t^2/\tau_2^2), \\ A_1 &= 2\sqrt{|\Phi_0|}\tau_2^2/[d(\tau_2^2 - \tau_1^2)], \\ A_2 &= \tau_1^2 A_1/\tau_2^2; \quad \tau_1^2 + \tau_2^2 = 3/|\Phi_0|; \\ \tau_1^2 &= (3 - \sqrt{9 - 3d/q})/2|\Phi_0|, \end{aligned} \quad (8)$$

where  $d$  and  $q$  are given in Eq. (6). The expression in Eq. (8) with  $A_1 = 1.267$ ,  $\tau_1 = 0.791$ ,  $A_2 = 0.067$ , and  $\tau_2 = 3.44$  is compared in Fig. 1(c) to a numerical integration along the potential contour with the value  $\Phi_0 = -0.2405$ , shown in Fig. 1(a). The approximation and numerical solution are indistinguishable over the time range shown.

The Lorentzian bifurcation leads to chaotic behavior if one or both of the parameters values  $b$  and  $c$  is modulated. As a specific example of chaotic behavior, contours of the amplitude  $y(t)$  are shown in Fig. 2 for the case that the value of parameter  $b$  is sinusoidally modulated over the range  $0.5 \leq b \leq 1.5$  at various frequencies. The frequency is scaled to  $f_s = b/2\pi c$  as the imaginary part of the eigenvalue at the fixed point  $b/c$  represents an angular frequency. Using the average value of  $b$ ,  $b = 1$ , and the fixed value of  $c$ ,  $c = 1$ ,  $f_s = 1/2\pi$  for this case. In Fig. 2, the dynamic behavior of  $y(t)$  at a fixed modulation frequency is given along a vertical line. A single Lorentzian pulse appears as a horizontal bar as, for example, at  $f/f_s = 0.50$ , while an extended series of pulses appears as a broken vertical line as, for example, at  $f/f_s = 0.183$ . All trajectories begin at the initial position,  $x = -20$ ,  $y = 0.01$ , and their temporal behavior is computed using fourth order Runge-Kutta numerical integration. The parameter  $b$  is

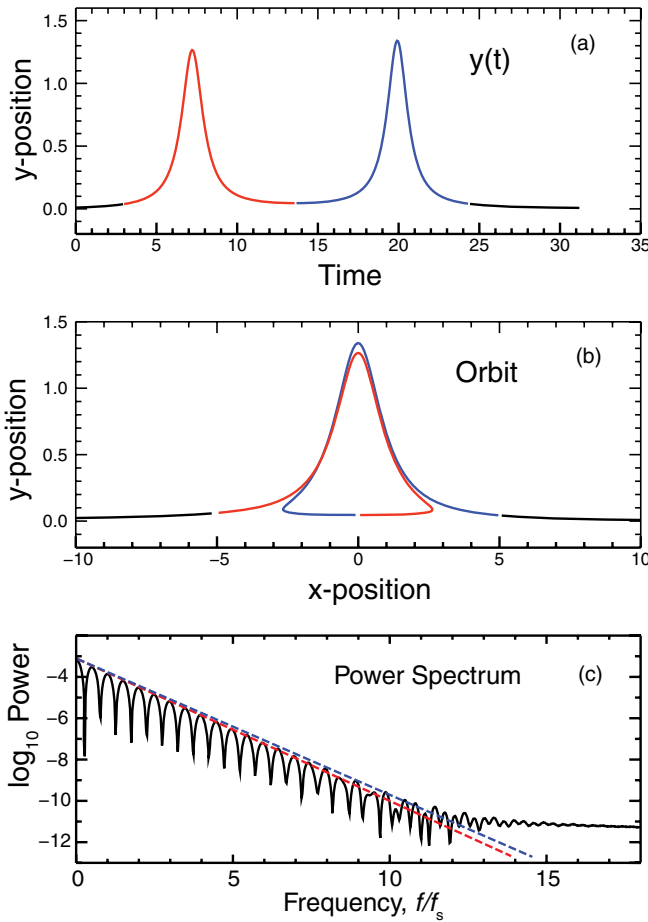


FIG. 3. (Color) (a) Details of the production of two Lorentzian pulses when parameter  $b$  is modulated at  $f = 0.1032 f_s$  (indicated by the red arrow in Fig. 2). (b) Lorentzian pulses are produced over the portion of the orbit that is in the immediate vicinity of the separatrix. (c) Power spectrum of the time signal is exponential (the two dashed curves are power spectra of the individual pulses).

modulated with frequencies in the range  $0 \leq f/f_s \leq 1.196$ . In the case that the parameter  $b$  is time independent, only a single Lorentzian pulse is produced in the time history of the trajectory for all values of  $0.5 \leq b \leq 1.5$ , similar to the behavior in the middle of the frequency range displayed in Fig. 2.

The details of the trajectory at the frequency indicated by the red arrow at the bottom of Fig. 2,  $f/f_s = 0.1032$ , are given in Fig. 3. At this frequency, two Lorentzian pulses are produced. At a frequency just below it,  $f/f_s = 0.0985$ , as seen in Fig. 2, 14 Lorentzian pulses are produced, so the dynamics are very sensitive to the modulation frequency, as is typical of chaotic behavior. The time signal is color-coded in Fig. 3(a) in order to show its relation to the orbit dynamics displayed in Fig. 3(b). Lorentzian pulses are produced by orbital motion in the immediate vicinity of the separatrix. Modulation of parameter  $b$  changes the location of the stationary point of the flow and thus the amplitude of the separatrix at  $x = 0$ . In the example shown in Fig. 3, the modulation allows trajectories to change topological character from unbounded to closed and back again, thus producing two Lorentzian pulses rather than one, as would occur in the absence of modulation. The fact that the Lorentzian pulses are created

near the separatrix is reflected in their widths and amplitudes. As indicated in Eq. (4), the width of the separatrix is  $\tau_s = c/b$ , and the amplitude is  $A_s = b/c^2$ . Since the value of parameter  $c$  is fixed ( $c = 1$  in this example) and the instantaneous width and amplitude of the separatrix are solely determined

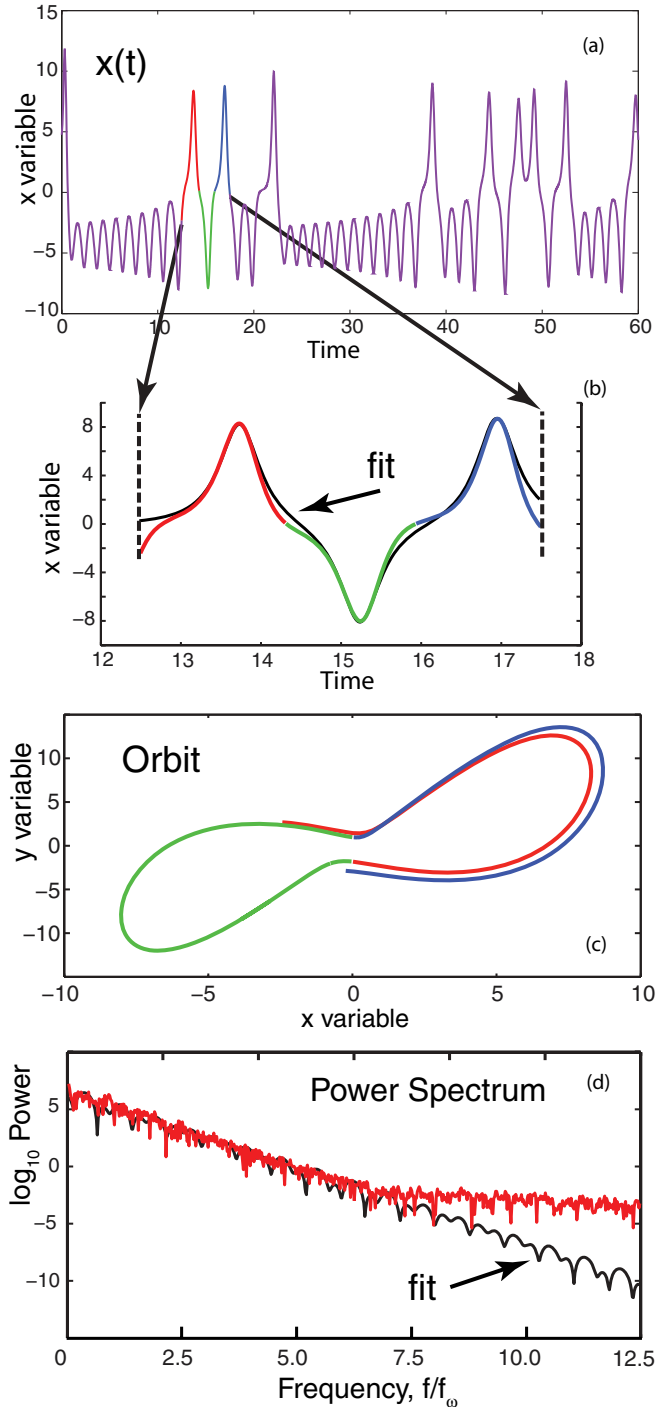


FIG. 4. (Color) (a) Time series for Lorenz model variable  $x$  shows intermittent pulses. (b) Color-coded time series is fit by a sum of three Lorentzian functions (black curve). (c) Phase-space trajectory of variables  $(y, x)$  is near the limit cycle of the attractor. (d) Frequency power spectrum of time series (red) compared to spectrum (black) of the sum of three Lorentzians.

by the value of  $b$ , the amplitude is inversely related to the width. For the two pulses shown in Fig. 3(a), the first pulse (red) has an amplitude  $A = 1.265$  ( $1/A = 0.795$ ) and width  $\tau = 0.794$ , and the second pulse (blue) has an amplitude  $A = 1.340$  ( $1/A = 0.745$ ) and width  $\tau = 0.760$ . The close relation between the inverse of the pulse amplitudes and their widths indicates that they reflect the state of the separatrix at the time of their formation. This occurs because the modulation frequency is a small fraction of the characteristic frequency at the fixed point ( $f = 0.1032 f_s$ ).

The flow field associated with the Lorentzian bifurcation transports (or advects) scalar quantities. If a scalar quantity in the vicinity of a Lorentzian bifurcation has a linear gradient in the  $y$  direction, then the Lorentzian nature of the  $y$  component of the trajectories leads to Lorentzian shaped pulses in the time signals of the advected scalar. This is the origin of the exponential power spectra in fluctuations of scalar quantities (such as density or temperature) observed in magnetically confined plasmas.

Very similar dynamical behavior occurs near the limit cycles of attractors in nonlinear dynamics models. Figure 4 illustrates the details of the production of Lorentzian pulses in the Lorenz model. Results are obtained from fourth order Runge-Kutta integration of the Lorenz model for the same parameters used in the comprehensive survey by Ohtomo *et al.* [11]. That study established that the different major mathematical models of deterministic chaos exhibit exponential frequency spectra, but the reason such spectra occur was not identified. The specific Lorenz parameters used are  $\sigma = 3$ ,  $r = 22$ , and  $b = 1$ . The integration time step used in this presentation,  $\Delta t = 0.005$ , is smaller than in Ref. [11]. Figure 4(a) displays the time series corresponding to the Lorenz variable  $x$  over the interval studied in Ref. [11]. The cursory interpretation is that, at this value of  $r$ , the system has entered the chaotic regime and exhibits intermittent pulses at seemingly random times. Figure 4(b) provides an expanded view of the sequence of three color-coded pulses bracketed by the arrows in Fig. 4(a). The color-coded portion of the trace (red, green, and blue) corresponds to the numerical solution. Superimposed on this solution is a black curve, which is the sum of three individual Lorentzian curves given by Eq. (1) with  $\tau = 0.3135$ , but with positive and negative amplitudes  $A$  as appropriate to each peak. The specific value of  $\tau$  corresponds to the expression  $\tau = \pi/2\omega$ , where  $\omega$  is the magnitude of the imaginary part of the complex eigenvalue of the Jacobian at the fixed points. For the Lorenz model, the two eigenvalues are complex conjugates with  $\omega = 5.01$ . It is evident that the

intermittent pulses follow a Lorentzian functional form. A similar conclusion is obtained by performing analogous fits to the other pulses in the time series as well as for other values of  $r$ . In all cases the widths of the Lorentzians generated are accurately determined by the imaginary part of the eigenvalue. Figure 4(c) corresponds to the  $(y, x)$  phase-space trajectory for the Lorenz model variables  $y$  and  $x$  over the time interval during which the Lorentzian pulses in Fig. 4(b) appear. The colors along the orbits correspond to those associated with the pulses in Figs. 4(a) and 4(b); they help identify that each Lorentzian-shaped pulse corresponds to one rotation around the boundary of the attractor. It is recognized from the display that these trajectories are near the limit cycle orbits around the two fixed points of the Lorenz attractors at  $y = x = \sqrt{b(r-1)} = \pm 4.5826$ . In displaying the power spectra in Fig. 4(d) the frequency is scaled to  $f_\omega$ , where  $2\pi f_\omega = \omega$ . The temporal width  $\tau$  of each Lorentzian is determined by the transit time around the attractor, and this in turn determines the slope (in a log-linear plot) of the exponential power spectrum, as illustrated in Fig. 4(d). In Fig. 4(d) the red curve corresponds to the power spectrum of the entire time series shown in Fig. 4(a), while the black curve is the power spectrum of the sum of the three Lorentzian functions that fit the intermittent pulses in Fig. 4(b). It is seen that the characteristic exponential spectrum associated with deterministic chaos is just the imprint of the Lorentzian pulses generated by the chaotic behavior of orbits near the limit cycle of the attractor. Analogous results are obtained for the average spectrum for a large ensemble of random initial values of the Lorenz variables  $(x, y, z)$ . Similar results connecting exponential spectra to Lorentzian pulses have also been obtained for the Duffing [24] and Rossler [25] models of deterministic chaos. Thus the property is robust.

In summary, Lorentzian pulses are a natural consequence of the chaotic dynamics in the vicinity of the separatrix of elliptic regions in potential flow fields or, analogously, the limit cycles of attractors in nonlinear dynamical models. The width of the Lorentzians is determined by the imaginary part of the complex eigenvalues of the underlying Jacobian matrix. These Lorentzian pulses are responsible for the exponential power spectra that characterize deterministic chaos and that are observed in a wide class of physical systems.

The work of J.E.M. and G.J.M. is performed under the auspices of the BaPSF at UCLA, which is jointly supported by a DOE-NSF cooperative agreement, and by DOE Grant No. SC0004663.

- 
- [1] J. E. Maggs and G. J. Morales, *Phys. Rev. Lett.* **107**, 185003 (2011).  
 [2] D. C. Pace, M. Shi, J. E. Maggs, G. J. Morales, and T. A. Carter, *Phys. Rev. Lett.* **101**, 085001 (2008).  
 [3] D. C. Pace, M. Shi, J. E. Maggs, G. J. Morales, and T. A. Carter, *Phys. Plasmas* **15**, 122304 (2008).  
 [4] G. Hornung, B. Nold, J. E. Maggs, G. J. Morales, M. Ramisch, and U. Stroth, *Phys. Plasmas* **18**, 082303 (2011).  
 [5] U. Frisch and R. Morf, *Phys. Rev. A* **23**, 2673 (1981).  
 [6] H. S. Greenside, G. Ahlers, P. C. Hohenberg, and R. W. Walden, *Phys. D* **5**, 322 (1982).  
 [7] A. Libchaber, S. Fauve, and C. Laroche, *Phys. D* **7**, 73 (1983).  
 [8] A. Brandstater and H. L. Swinney, *Phys. Rev. A* **35**, 2207 (1987).  
 [9] C. L. Streett and M. Y. Hussaini, *Appl. Numer. Math.* **7**, 41 (1991).  
 [10] D. E. Segeti, *Phys. D* **82**, 136 (1995).

- [11] N. Ohtomo, K. Tokiwano, Y. Tanaka, A. Sumi, S. Terachi, and H. Konno, *J. Phys. Soc. Jpn.* **64**, 1104 (1995).
- [12] B. Mensour and A. Longtin, *Phys. D* **113**, 1 (1998).
- [13] M. R. Paul, M. C. Cross, P. F. Fischer, and H. S. Greenside, *Phys. Rev. Lett.* **87**, 154501 (2001).
- [14] A. Bershadskii, *Europhys. Lett.* **85**, 49002 (2009).
- [15] A. Bershadskii, *J. Cosmol.* **8**, 1893 (2010).
- [16] D. S. Andres, D. F. Cerquetti, and M. Merello, *J. Neurosci. Methods* **197**, 14 (2011).
- [17] H. G. Schuster and W. Just, *Deterministic Chaos* (Wiley-VCH, Weinheim, Germany, 2005).
- [18] J. A. Boedo, D. Rudakov, R. Moyer, S. Krasheninnikov, D. Whyte, G. McKee, G. Tynan, M. Schaffer, P. Stangeby, P. West, S. Allen, T. Evans, R. Fonck, E. Hollmann, A. Leonard, A. Mahdavi, G. Porter, M. Tillack, and G. Antar, *Phys. Plasmas* **8**, 4826 (2001).
- [19] G. Y. Antar, G. Counsell, Y. Yu, B. Labombard, and P. Devynck, *Phys. Plasmas* **10**, 419 (2003).
- [20] F. Sattin, M. Agostini, R. Caravazzana, P. Scarin, and J. L. Terry, *Plasma Phys. Controlled Fusion* **51**, 095004 (2009).
- [21] D. A. D'Ippolito, J. R. Myra, and S. J. Zweben, *Phys. Plasmas* **18**, 060501 (2011).
- [22] E. N. Lorenz, *J. Atmos. Sci.* **20**, 130 (1963).
- [23] T. Miloh and M. P. Tulin, *J. Phys. A* **22**, 921 (1989).
- [24] *The Duffing Equation: Nonlinear Oscillators and Their Behavior*, edited by I. Kovacic and M. J. Brennan (Wiley, Chichester, UK, 2011).
- [25] O. E. Rossler, *Phys. Lett. A* **57**, 397 (1976).